AGU PUBLICATIONS

Geophysical Research Letters

RESEARCH LETTER
10.1002/2014GL061481

Key Points:
- Peak mass deposition rate is mass flux/(e × neutral scale height)
- Peak occurs where dust half the radius of largest particle is ablated
- Results are useful for preencounter predictions and postencounter analysis

Correspondence to:
P. Withers,
withers@bu.edu

Citation:
Withers, P. (2014), Predictions of the effects of Mars's encounter with comet C/2013 A1 (Siding Spring) upon metal species in its ionosphere, *Geophys. Res. Lett.*, *41*, doi:10.1002/2014GL061481.

Received 8 AUG 2014
Accepted 16 SEP 2014
Accepted article online 18 SEP 2014

Predictions of the effects of Mars's encounter with comet C/2013 A1 (Siding Spring) upon metal species in its ionosphere

Paul Withers[1,2]

[1]Department of Astronomy, Boston University, Boston, Massachusetts, USA, [2]Center for Space Physics, Boston University, Boston, Massachusetts, USA

Abstract The infall of dust from the coma of comet C/2013 A1 (Siding Spring) and its subsequent ablation in the atmosphere of Mars has the potential to affect the abundances of metal species in the atmosphere and ionosphere. We develop relationships between properties of the dust population in the coma and densities of metal species in the atmosphere and ionosphere. These can be used to predict the abundances of metal species in the atmosphere and ionosphere during the encounter. Given postencounter observations of the atmosphere and ionosphere, they can also be used to infer relevant cometary properties. Although current predictions suggest that the influx of cometary dust will be comparable to the sporadic background, the higher entry speed involved, which leads to a greater production rate of ions during ablation, means that metal ion abundances may be enhanced during and after the encounter.

1. Introduction

Mars will experience a remarkably close encounter with comet C/2013 A1 (Siding Spring) on 19 October 2014 at a close approach distance of approximately 135,000 km [*Yelle et al.*, 2014; *Tricarico et al.*, 2014]. During this encounter, the flux of interplanetary dust particles onto Mars may increase somewhat. Estimates of this increase range from practically zero [*Ye and Hui*, 2014; *Tricarico et al.*, 2014] to more than 4 orders of magnitude [*Moorhead et al.*, 2014; *Moores et al.*, 2014].

The ablation of interplanetary dust in planetary upper atmospheres introduces metal species into these atmospheres [*Grebowsky et al.*, 2002]. This is the primary source of metal species in planetary upper atmospheres. When these metal species can become ionized, they tend to form long-lived atomic ions, and hence metal ions can give rise to noticeable features in planetary ionospheres [*Molina-Cuberos et al.*, 2008]. Indeed, layers of ions inferred to be metal ions have been observed sporadically at altitudes of ~90 km and densities of 10^{10} m^{-3} on Mars [*Pätzold et al.*, 2005; *Withers et al.*, 2008], distinctly below the two main layers of the ionosphere that are composed of O_2^+ ions, occur at altitudes of ~110 km and ~130 km and have densities on the order of 10^{11} m^{-3} [*Withers*, 2009].

It is therefore worthwhile to consider whether possible increases in the dust flux during the cometary encounter will affect the ionosphere of Mars.

We aim to develop relationships between properties of the dust population in the cometary coma and densities of metal species in the atmosphere and ionosphere of Mars. These relationships will serve two purposes. First, given preencounter estimates of relevant cometary properties, they can be used to predict the abundances of metal species in the atmosphere and ionosphere during the encounter. Second, given postencounter observations of the atmosphere and ionosphere, they can be used to infer relevant cometary properties.

We combine a model of the dust population in the coma (section 2), a model of the ablation of dust particles in the atmosphere of Mars (section 3), and a model of the chemistry of metal species in the ionosphere of Mars (section 4) to predict the injection rate of metal species into the atmosphere and the associated density of metal ions in the ionosphere. Predictions of other effects of this encounter on the atmosphere of Mars have been made by *Moores et al.* [2014] and *Yelle et al.* [2014].

Given the uncertainties that exist regarding many critical properties of dust in the cometary coma, we use relatively simple models at each step, rather than striving for the most comprehensive model possible.

This choice results in closed-form analytic expressions for the mass flux of dust particles onto Mars and for vertical profiles of related quantities. We illustrate the results of this work using benchmark values of cometary properties. These benchmark values are essentially those of the model of *Moorhead et al.* [2014], updated to reflect an improved estimate for the absolute magnitude of the comet and to correct an erroneous value for the maximum mass of a dust particle. The suitability of these values, and of the models themselves, is discussed in section 5. Potential methods by which metal species can be observed in the atmosphere and ionosphere are outlined in section 6. Our conclusions are summarized in section 7.

2. Dust Population

Moorhead et al. [2014] introduced an analytical model for the dust population in a cometary coma. If the size distribution of dust particles is given by $f(s) = C\left(s/s_0\right)^{-k}$, where C is a constant, s is dust particle radius, s_0 is a reference radius, and k is an exponent, then the total number of dust particles in the coma, N_{tot}, satisfies

$$N_{\mathrm{tot}} = \int_{s_{\mathrm{min}}}^{s_{\mathrm{max}}} f(s)\mathrm{d}s \tag{1}$$

Here s_{min} and s_{max} are the minimum and maximum dust particle radii, respectively. The total mass of dust particles in the coma, M_{tot}, satisfies

$$M_{\mathrm{tot}} = \int_{s_{\mathrm{min}}}^{s_{\mathrm{max}}} f(s)\frac{4\pi\rho s^3}{3}\mathrm{d}s \tag{2}$$

Here ρ is the mass density of a dust particle. The constant C in the size distribution can be constrained by the comet's brightness [*Moorhead et al.*, 2014]:

$$C = \left(\frac{g\,(1\ \mathrm{AU})^2\ 10^{-0.4\left(M1-m_{\mathrm{Sun,1\ AU}}\right)}}{a\,(h/1\ \mathrm{AU})^{\beta}}\right)\left(\frac{3-k}{s_0^3}\right)\left(\frac{s_0}{s_{\mathrm{min}}}\right)^{3-k}\left(\frac{1}{\left(\frac{s_{\mathrm{max}}}{s_{\mathrm{min}}}\right)^{3-k}-1}\right) \tag{3}$$

Here g is the fractional dust contribution to the comet's total brightness, a is the dust albedo, h is the heliocentric distance, β is an exponent, $M1$ is the comet's absolute magnitude, and $m_{\mathrm{Sun,1\ AU}}$ is the apparent magnitude of the Sun at 1 AU. Hence, N_{tot} and M_{tot} satisfy

$$N_{\mathrm{tot}} = \left(\frac{1}{s_{\mathrm{min}}^2}\right)\left(\frac{g\,(1\ \mathrm{AU})^2\ 10^{-0.4\left(M1-m_{\mathrm{Sun,1\ AU}}\right)}}{a\,(h/1\ \mathrm{AU})^{\beta}}\right)\left(\frac{3-k}{1-k}\right)\left(\frac{\left(\frac{s_{\mathrm{max}}}{s_{\mathrm{min}}}\right)^{1-k}-1}{\left(\frac{s_{\mathrm{max}}}{s_{\mathrm{min}}}\right)^{3-k}-1}\right) \tag{4}$$

$$M_{\mathrm{tot}} = \left(\frac{4\pi\rho s_{\mathrm{min}}}{3}\right)\left(\frac{g\,(1\ \mathrm{AU})^2\ 10^{-0.4\left(M1-m_{\mathrm{Sun,1\ AU}}\right)}}{a\,(h/1\ \mathrm{AU})^{\beta}}\right)\left(\frac{3-k}{4-k}\right)\left(\frac{\left(\frac{s_{\mathrm{max}}}{s_{\mathrm{min}}}\right)^{4-k}-1}{\left(\frac{s_{\mathrm{max}}}{s_{\mathrm{min}}}\right)^{3-k}-1}\right) \tag{5}$$

If $k < 3$ and $s_{\mathrm{max}} \gg s_{\mathrm{min}}$, then the last term on the right-hand side of equation (5) reduces to $s_{\mathrm{max}}/s_{\mathrm{min}}$ so that M_{tot} is proportional to s_{max} and independent of s_{min}.

The number density, ν, of dust particles is assumed to follow $\nu(r) = Dr^{-2}$, where r is cometocentric distance and D is a constant. Assuming that the coma extends from $r = 0$ to $r = r_c$, where r_c is the coma radius, integration of the number density over the volume of the coma gives $N_{\mathrm{tot}} = 4\pi D r_c$. Once N_{tot} is determined by the cometary brightness via equation (4) and r_c is specified, the values of D and the number density at any cometocentric distance are also determined. Adoption of parameter values from Table 1 gives values for N_{tot} and M_{tot} of 1.7×10^{17} and 3.1×10^{9} kg, respectively. The validity of these numerical results is addressed in section 5.

For a Mars-comet distance of r, where $r < r_c$, and relative speed v_{rel}, the flux of dust particles incident upon Mars (number per unit area per unit time) is Dv_{rel}/r^2. The mass flux of dust particles is the product of this

Table 1. Nominal Values of Input Parameters

Parameter	Symbol	Value	Source
Size distribution exponent	k	2.6	*Fulle et al.* [2000]
Minimum dust particle mass	m_{min}	10^{-12} kg	*Fulle et al.* [2000]
Maximum dust particle mass[a]	m_{max}	10^{-3} kg	*Fulle et al.* [2000]
Mass density of dust particles	ρ	10^2 kg m^{-3}	*Fulle et al.* [2000]
Minimum dust particle radius	s_{min}	1.3×10^{-5} m	ρ and m_{min}
Maximum dust particle radius	s_{max}	1.3×10^{-2} m	ρ and m_{max}
Dust contribution fraction	g	1	*Moorhead et al.* [2014]
Dust particle albedo	a	0.04	*Fulle et al.* [2000]
Heliocentric distance	h	1.4 AU	*Moorhead et al.* [2014]
Heliocentric distance exponent	β	2.4	*Moorhead et al.* [2014]
Absolute magnitude of comet	$M1$	8.6	Jet Propulsion Laboratory (JPL) Small Bodies Database[b]
Apparent magnitude of the Sun at 1 AU	$m_{Sun,1\ AU}$	−26.74	*Moorhead et al.* [2014]
Radius of coma	r_c	2×10^8 m	*Moorhead et al.* [2014]
Closest approach distance to Mars	r	1.35×10^8 m	JPL Small Bodies Database[b]
Speed of comet relative to Mars	v_{rel}	5.6×10^4 m s^{-1}	JPL Small Bodies Database[b]
Dimensionless drag coefficient	Γ	0.75	*Pesnell and Grebowsky* [2000]
Dimensionless shape factor	A	1.21	*Hughes* [1992]
Sputtering efficiency	Λ	1	*Molina-Cuberos et al.* [2003]
Latent heat of ablation	Q	7×10^6 J kg^{-1}	*Pesnell and Grebowsky* [2000]
Atmospheric density at surface	ρ_{a0}	4.1×10^{-2} kg m^{-3}	*Seiff and Kirk* [1977]
Neutral scale height	H	8.2×10^3 m	*Seiff and Kirk* [1977]
Mass fraction of Mg	ϵ	0.143	*Pesnell and Grebowsky* [2000]
Characteristic velocity for ionization	v_L	9.4×10^4 m s^{-1}	*Lebedinets et al.* [1973]

[a]*Moorhead et al.* [2014] adopt dust parameters from the model of *Fulle et al.* [2000], which is based on Giotto data from comets 1P/Halley and 26P/Grigg-Skjellerup, but, in an apparent error of transcription, adopt a maximum mass of 3.1 × 10^{-2} kg that is 2 orders of magnitude larger than the heaviest particle detected by Giotto [*Pätzold et al.*, 1993a, 1993b; *Fulle et al.*, 2000] and more than an order of magnitude outside than the applicable mass range reported by *Fulle et al.* [2000] for their model.
[b]http://ssd.jpl.nasa.gov/sbdb.cgi.

and the average mass, which is equal to M_{tot}/N_{tot}. Since $N_{tot} = 4\pi D r_c$, it follows that the mass flux Φ (mass per unit area per unit time) satisfies

$$\Phi = \frac{M_{tot} v_{rel}}{4\pi r_c r^2} \tag{6}$$

Adoption of parameter values from Table 1 gives a mass flux at closest approach of 3.8×10^{-12} kg m^{-2} s^{-1} or, integrating over the exposed hemisphere of Mars, a rate of 140 kg s^{-1}. The mass accretion rate under normal circumstances is on the order of 0.01 kg s^{-1}, 4 orders of magnitude smaller [*Moores et al.*, 2014]. The validity of these numerical results is addressed in section 5.

3. Deposition of Dust in the Atmosphere

Dust particles incident upon Mars will ablate as they enter the atmosphere at orbital speeds. During its atmospheric entry, the speed V and mass m of a dust particle satisfy [*Hughes*, 1992]:

$$\frac{dv}{dt} = -\frac{\Gamma A \rho_a v^2}{m^{1/3} \rho^{2/3}} \tag{7}$$

$$\frac{dm}{dt} = -\frac{\Lambda A m^{2/3} \rho_a v^3}{2Q\rho^{2/3}} \tag{8}$$

where t is time, Γ is a dimensionless drag coefficient, A is a dimensionless shape factor, ρ_a is the mass density of the atmosphere, Λ is a dimensionless heat transfer coefficient, and Q is the latent heat of ablation of dust particles. Here we have assumed vertical incidence for simplicity. More comprehensive versions of these equations exist [*Pesnell and Grebowsky*, 2000; *Molina-Cuberos et al.*, 2003; *Whalley and Plane*, 2010], but they

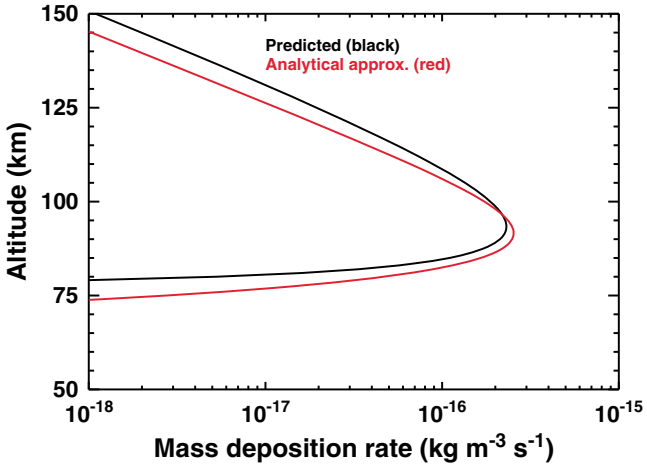

Figure 1. Vertical profile of the mass deposition rate $\Psi(z)$ that results from the ablation of cometary dust particles in the atmosphere of Mars (black line). Input parameters, which are taken from Table 1, are discussed in section 5. The analytical approximation to $\Psi(z)$ is also shown (red line).

are not necessary for this work. Eliminating time from equations (7) and (8) and integrating leads to [*Hughes*, 1992]

$$m = m_\infty \exp\left(\frac{\Lambda}{4Q\Gamma}\left(v^2 - v_\infty^2\right)\right) \quad (9)$$

Here m_∞ and v_∞ are the preentry mass and speed of the dust particle, where $v_\infty = v_{rel}$. Since $v = -\mathrm{d}z/\mathrm{d}t$, where z is altitude, equation (7) can be written as

$$\frac{\mathrm{d}v}{\mathrm{d}z} = \frac{\Gamma A \rho_a(z) v(z)}{m(z)^{1/3}\rho^{2/3}} \quad (10)$$

This can be expressed purely in terms of altitude z by assuming an exponential atmosphere, $\rho_a = \rho_{a0}\exp(-z/H)$, where ρ_{a0} is $\rho(0)$ and H is a scale height, and using equation (9) to eliminate $m(z)$.

$$\frac{\Gamma A \rho_{a0}}{m_\infty^{1/3}\rho^{2/3}}\exp(-z/H)\,\mathrm{d}z = \frac{\mathrm{d}v}{v}\exp\left(\frac{\Lambda}{12Q\Gamma}\left(v^2 - v_\infty^2\right)\right) \quad (11)$$

The function $v(z)$ satisfies

$$\frac{\Gamma A \rho_{a0} H}{m_\infty^{1/3}\rho^{2/3}}\exp(-z/H) = \int_{v'=v}^{v'=v_\infty}\frac{\mathrm{d}v'}{v'}\exp\left(\frac{\Lambda}{12Q\Gamma}\left(v'^2 - v_\infty^2\right)\right) \quad (12)$$

Once equation (12) has been solved numerically for $v(z)$, equation (9) yields $m(z)$. The function thereby obtained describes how the mass of a dust particle with preentry mass of m_∞ decreases due to ablation as altitude decreases. Multiplication of the derivative $\mathrm{d}m/\mathrm{d}z$ (kg m^{-1}) by the flux of particles with preentry masses in the range m_∞ to $m_\infty + \delta m$ (m^{-2} s^{-1}), followed by integration over the entire size distribution function, yields the mass deposition rate per unit volume (kg m^{-3} s^{-1}) of cometary dust in the atmosphere, $\Psi(z)$. This is shown in Figure 1, where parameter values were adopted from Table 1. The maximum mass deposition rate per unit volume, 1.6×10^{-16} kg m^{-3} s^{-1}, occurs at 93 km altitude. The validity of these numerical results is addressed in section 5.

This result for $\Psi(z)$ requires numerical integration to find $v(z)$, followed by numerical integration over the size distribution. It is desirable to find an analytical approximation to the function $\Psi(z)$ so that predictions can be updated easily in response to revised input parameters. An analytical approximation will also be useful for identifying how each input parameter influences $\Psi(z)$. An analytical approximation to $\Psi(z)$ can be found as follows.

The function $\Psi(z)$ will be most strongly influenced by the behavior of particles of radius s_{crit}, where particles larger than s_{crit} deliver half the mass flux. That is,

$$\int_{s_{min}}^{s_{max}} f(s)\frac{4\pi\rho s^3}{3}\mathrm{d}s = 2\int_{s_{crit}}^{s_{max}} f(s)\frac{4\pi\rho s^3}{3}\mathrm{d}s \quad (13)$$

Since $f(s) = C\left(s/s_0\right)^{-k}$, the smallest particles have negligible effect on the mass flux when $k < 3$. Hence, s_{min} can be approximated as zero here, which leads to

$$\int_0^{s_{max}} s^{3-k}\mathrm{d}s = 2\int_{s_{crit}}^{s_{max}} s^{3-k}\mathrm{d}s \quad (14)$$

Thus, $s_{crit}/s_{max} = 2^{1/(k-4)}$. For $k = 2.6$ (Table 1), $s_{crit}/s_{max} = 0.61$.

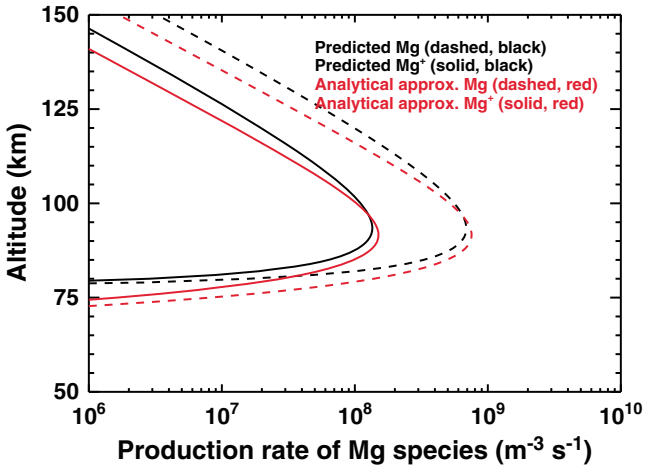

Figure 2. Vertical profiles of the production rates of neutral Mg atoms (dashed black line) and Mg^+ ions (solid black line). Input parameters, which are taken from Table 1, are discussed in section 5. The corresponding analytical approximations are also shown (red lines).

The ablation of a particle of radius s_{crit}, which has a preentry mass of m_{crit}, is centered on the altitude z_{crit} where the atmospheric density is ρ_{crit}. This critical atmospheric density can be found by combining equation (8) and $v = -dz/dt$ to obtain

$$\frac{dm}{dz} = \frac{\Lambda A m^{2/3} \rho_a v^2}{2Q\rho^{2/3}} \quad (15)$$

If, in equation (15), $-dm$ and m are equated to m_{crit}, $-dz$ to H, and v to v_{rel}, then the inferred value of ρ_a is an estimate for ρ_{crit}.

$$\rho_{crit} = \frac{2m_{crit}^{1/3} Q\rho^{2/3}}{H\Lambda A v_{rel}^2} \quad (16)$$

The shape of the function $\Psi(z)$ can be assumed to be that of a Chapman function with width H and peak altitude z_{crit}. The Chapman function, which is found in many aspects of aeronomy, is $Ch(y) = \exp(1 - y - \exp(-y))$, where $y = (z - z_{crit})/H$. Since the column-integrated mass deposition rate must equal the incident mass flux, we have $\Psi = \Phi Ch(y)/eH$. Figure 1 shows that this estimate for Ψ is consistent with the result of the more comprehensive and more complicated integration across the size distribution function. The maximum mass deposition rate per unit volume from the analytical approximation to $\Psi(z)$, $\Phi/eH = 1.7 \times 10^{-16}$ kg m^{-3} s^{-1}, is within 10% of the actual value of 1.6×10^{-15} kg m^{-3} s^{-1} and the estimated altitude of this maximum, 92 km, differs from the actual altitude of 93 km by much less than one scale height (8.2 km).

4. Ionospheric Response

In keeping with prior simulations of the effects of ablated dust particles on the ionosphere of Mars, we focus on one species, Mg [*Pesnell and Grebowsky*, 2000; *Molina-Cuberos et al.*, 2003; *Whalley and Plane*, 2010]. This is abundant (14.3% by mass for chondritic composition, $\epsilon = 0.143$), readily ionized, and otherwise absent from the upper atmosphere [*Pesnell and Grebowsky*, 2000]. The number of Mg atoms injected into the atmosphere per unit volume per unit time is simply the ratio of $\epsilon\Psi(z)$ to the atomic mass of Mg, m_{Mg}.

The fraction of these atoms that are directly ionized during ablation depends on the speed of the dust particle at the time of ablation [*Molina-Cuberos et al.*, 2008]. The fraction of atoms ablated from a dust particle of speed v that are ionized is $\beta = (v/v_L)^{7/2}$, where v_L equals 9.4×10^4 m s^{-1} [*Lebedinets et al.*, 1973]. At the onset of ablation, when $v = v_{rel}$, $\beta = 0.17$. Given this relationship for β, the number of Mg^+ ions injected into the atmosphere per unit volume per unit time can be calculated. The production rate of Mg^+ ions can also be estimated from the analytical approximation to $\Psi(z)$ by using the value of β for $v = v_{rel}$ at all altitudes. This estimated production rate of Mg^+ ions is $\epsilon\,\Psi(z)\,(v_{rel}/v_L)^{7/2}\, m_{Mg}^{-1}$. The predicted production rates of neutral Mg atoms and Mg^+ ions are shown in Figure 2 alongside the corresponding analytical approximations.

Given the input parameters listed in Table 1, the peak production rates of neutral Mg atoms and of Mg^+ ions are 4.7×10^8 m^{-3} s^{-1} and 9.1×10^7 m^{-3} s^{-1}, respectively, at 93 km. If the analytical approximation to $\Psi(z)$ is used, then these values are 5.1×10^8 m^{-3} s^{-1} and 1.0×10^8 m^{-3} s^{-1}, respectively. For reference, simulations of the production rate under normal conditions have reported values of 10^4–10^5 m^{-3} s^{-1} for neutral atoms and 10 m^{-3} s^{-1} for ions [*Pesnell and Grebowsky*, 2000; *Molina-Cuberos et al.*, 2003; *Whalley and Plane*, 2010].

Accurate calculation of the vertical profile of the number density of Mg^+ ions during the cometary encounter requires sophisticated chemical models [*Pesnell and Grebowsky*, 2000; *Molina-Cuberos et al.*, 2003; *Whalley and Plane*, 2010] that are capable of handling time-dependent production rates of metal species. Such models are beyond the scope of this work. However, the Mg^+ number density can be estimated to

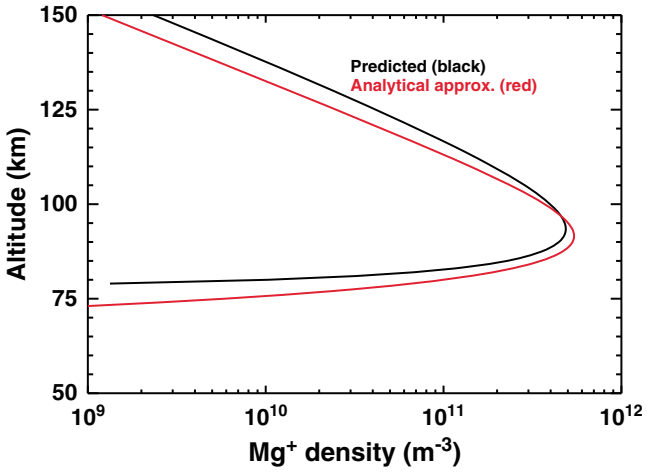

Figure 3. Vertical profile of the number density of Mg^+ ions (black line). Input parameters, which are taken from Table 1, are discussed in section 5. The analytical approximation to this result is also shown (red line).

be on the order of the product of the production rate of Mg^+ ions and a timescale, where the timescale is the shorter of the duration of the encounter and the Mg^+ ion lifetime. Note that this estimate assumes that the only mechanism for producing Mg^+ ions is direct ionization during ablation, and it therefore neglects ions produced from Mg atoms by photoionization or charge exchange. To estimate Mg^+ densities, we shall assume that the duration of the encounter is shorter than the Mg^+ ion lifetime, then check the validity of this assumption.

During the encounter, enhanced dust influx will persist for on the order of 1 h [*Yelle et al.*, 2014; *Ye and Hui*, 2014; *Tricarico et al.*, 2014]. The Mg^+ ion densities estimated using the duration of the encounter as the timescale are shown in Figure 3. Inspection of Figure 12 of *Whalley and Plane* [2010] shows that the Mg^+ ion lifetimes associated with these estimated densities are longer than the duration of the encounter, which confirms that it is appropriate to use the duration of the encounter, rather than the ion lifetime, to estimate ion densities. The peak estimated density in Figure 3 exceeds the densities of 10^{10} m^{-3} seen to date in metal ion layers on Mars by 2 orders of magnitude. It also exceeds the typical subsolar peak density of the ionosphere (2×10^{11} m^{-3}). The validity of this numerical result is addressed in section 5.

In this model, the peak production rate of Mg atoms is 4 orders of magnitude greater than that predicted by *Whalley and Plane* [2010] for normal conditions. This raises the question of why the ion densities predicted in this work are not even larger. The answer lies in the brief duration of the encounter. The encounter does not last long enough for the elevated Mg production rate to increase ion densities from their background values to their corresponding elevated steady state values. If the Mg^+ ion densities are instead estimated as the product of the production rate and 10^5 s, a representative ion lifetime from *Whalley and Plane* [2010], then estimated ion densities would be much higher, on the order of 10^{13} m^{-3}, which greatly exceeds the typical subsolar peak density of the ionosphere of 2×10^{11} m^{-3}.

Using the duration of the encounter as the appropriate timescale, the analytical approximation to the peak Mg^+ density is

$$Mg^+_{max} = \frac{\epsilon M_{tot} v_{rel}}{4\pi e H r_c r^2 m_{Mg}} \times (\text{duration of encounter}) \quad (17)$$

where r is the closest approach distance and m_{Mg} is the atomic mass of Mg. The corresponding peak altitude is the altitude of maximum mass deposition rate.

5. Caveats

Taken at face value, section 4 predicts that the encounter of comet C/2013 A1 (Siding Spring) with Mars will increase the density of metal ions in its ionosphere by more than an order of magnitude, with the potential to drastically perturb the structure of the lower ionosphere. Should these predictions be believed?

The predictions outlined here are based on a succession of simple models (dust population, dust ablation, and chemistry of metal species). None of them should be considered comprehensive. The results are not particularly sensitive to the assumed value of m_{min}. However, for each order of magnitude increase in m_{max}, the mass flux and peak deposition rate increase by a factor of 2 and the altitude of peak ablation drops by 6 km. If the density of a dust particle is increased by 1 order of magnitude, then the mass flux and peak deposition rate increase by a factor of 5 and the altitude of peak ablation drops by 12 km.

In this model, r_c plays a crucial role. If we adopt a value for r_c that equals the close approach distance, then the numerical results of the previous sections only change by a factor of 2. If we adopt a value for r_c that is slightly less than the close approach distance, then no deposition of dust into the atmosphere is predicted at all.

Estimates of the mass flux of cometary dust onto Mars suggest that the peak flux will be in the range of "practically indistinguishable from the background" [*Ye and Hui*, 2014; *Tricarico et al.*, 2014] to "more than four orders of magnitude greater than the background" [*Moorhead et al.*, 2014; *Moores et al.*, 2014]. The most reliable estimates are likely to be those based on the most recent observations of comet C/2013 A1 (Siding Spring) and on the most physically realistic models of dust activity. These estimates suggest minimal accretion of cometary dust by Mars during the encounter and imply that changes in the abundances of metal species in the atmosphere and ionosphere and in overall plasma densities may be negligible. Hence, the numerical values predicted in the earlier sections of this work should not be taken literally.

Nevertheless, the comet's activity could increase unexpectedly prior to its encounter with Mars and the possibility of accretion of appreciable amounts of metal species cannot be completely excluded. Therefore, the relationships developed in this work will be useful prior to the encounter for updating predictions of the abundances of metal species if cometary properties change. They will also be useful after the encounter for reconciling disparate observations of cometary and Martian properties.

Moreover, the 56 km s^{-1} entry speed of dust from comet C/2013 A1 (Siding Spring) is exceptionally fast. Of the predicted Martian meteor showers listed by *Jenniskens* [2006], only that associated with comet 1P/Halley has a greater speed. For cometary dust entering at 56 km s^{-1}, 17% of ablated Mg atoms are directly ionized. For slower sporadic dust particles entering at 10 km s^{-1}, fewer than 0.05% are directly ionized [*Pesnell and Grebowsky*, 2000]. Consequently, a mass flux of cometary dust identical to the sporadic background will more than double the normal Mg^+ density.

The discrepancy between the early dust predictions of *Moorhead et al.* [2014] and those made later by *Ye and Hui* [2014] and *Tricarico et al.* [2014] is readily explained. *Moorhead et al.* [2014] assumed, based on comet C/2013 A1 (Siding Spring) being considered a "new, highly active Oort cloud comet", a nominal coma radius of 200,000 km, which is twice that of 1P/Halley. Subsequent observations of the comet revealed that its dust activity is characterized by an ejection velocity on the order of 1 m s^{-1} [*Ye and Hui*, 2014; *Tricarico et al.*, 2014]. If all other forces acting on the dust particles are neglected, a dust particle ejected at 1 m s^{-1} will take over 4 years to separate from the nucleus by 135,000 km. Since the comet came within 7 AU of the Sun for the first time in January 2013, this suggests that the radius of the coma will be significantly smaller than the nominal value of 200,000 km used by *Moorhead et al.* [2014] and that few cometary dust particles will impact Mars. *Ye and Hui* [2014] estimate that the coma radius will be approximately 70,000 km at the time of the encounter with Mars.

If the dust number density at closest approach, $\nu(b)$, is measured directly by spacecraft during the encounter, then prediction of the abundances of metal species in the atmosphere and ionosphere does not require a specific dust population model (section 2). Instead, the analytical approximation to the mass deposition rate, $\Psi(z)$, can be written as $m_{av}\nu(b)v_{rel}Ch(y)/eH$, where m_{av} is the average mass of a dust particle (i.e., M_{tot}/N_{tot}).

6. Potential Observations

There are several methods by which the effects of the ablation of cometary dust in the atmosphere of Mars may be observed. Radio occultations by Mars Express, Mars Reconnaissance Orbiter, and other Mars orbiters can acquire vertical profiles of ionospheric electron density. The Mars Advanced Radar for Subsurface and Ionosphere Sounding (MARSIS) topside radar sounder on Mars Express can acquire vertical profiles of ionospheric electron density down to the altitude of maximum electron density, accompanied by very direct measurements of the maximum electron density. MARSIS and the Shallow Subsurface Radar (SHARAD) on Mars Reconnaissance Orbiter can measure the vertical column-integrated electron density, which is generally proportional to the maximum electron density. Ultraviolet spectrometer observations by the MAVEN spacecraft may be able to detect resonance lines from Mg and Mg^+ at 285 nm and 280 nm [*Whalley and Plane*, 2010], respectively, amidst a background of dayglow emissions from CO_2^+ ions. In situ measurements by MAVEN's ion and neutral mass spectrometer (the NGIMS instrument), Langmuir probe (the LPW

instrument), and thermal ion spectrometer (the STATIC instrument) will have the potential to detect metal ions, metal neutrals, and enhanced plasma densities, although they will be restricted to altitudes above the MAVEN periapsis at 150 km. Finally, increased amounts of neutral sodium, another metal, in the atmosphere will increase the resonant scattering of sunlight from the sodium D lines, which may be detectable by ground-based imaging [*Barbier and Roach*, 1949]. However, optical emissions from atmospheric "sodium layers" on another planet has not been observed to date.

7. Conclusions

The mass flux (kg m^{-2} s^{-1}) onto Mars during the encounter equals $m_{av}v(r)v_{rel}$. According to the model of *Moorhead et al.* [2014], in which the number density of dust in the coma decreases with the inverse square of distance from the nucleus, this is $M_{tot}v_{rel}/\left(4\pi r_c r^2\right)$ where $r < r_c$ and zero where $r > r_c$.

The vertical profile of mass deposition rate (kg m^{-3} s^{-1}) can be reasonably approximated by a Chapman layer shape controlled by the neutral scale height, H. The peak mass deposition rate is the ratio of the mass flux to eH. The altitude of the peak mass deposition rate is the altitude at which particles of radius s_{crit} are ablated, where particles larger than s_{crit} deliver half the mass flux. For size distributions characterized by an exponent k that is less than 3, s_{crit} is on the order of half the radius of the largest dust particle in the population. That is, the corresponding mass m_{crit} is approximately 1 order of magnitude smaller than the mass of the largest dust particle in the population. The atmospheric density at which the mass deposition rate peaks is proportional to the latent heat of ablation of a dust particle, to the one-third power of m_{crit}, to the two-thirds power of the mass density of a dust particle, and inversely proportional to the neutral scale height (equation (16)).

The number density of Mg^+ ions can be estimated as the product of the production rate of Mg^+ ions and the duration of the encounter. The ion lifetime is not present in this expression because the ion lifetime is much longer than the duration of the encounter. Even given a prediction of greatly enhanced production rates of Mg^+ ions at closest approach, the encounter is too short for these enhanced rates to increase ion densities from their background values to their corresponding steady state values. If metal ion densities are increased during the encounter, then they should remain above background levels for hours to days after the encounter.

The high speed of cometary dust relative to the sporadic dust means that a much higher fraction of ablated metal atoms will be directly ionized during the encounter than usual. This factor will increase metal ion densities even if the cometary dust flux is not significantly larger than the sporadic background. Although sophisticated models of the chemistry of metal species in the atmosphere of Mars do exist, it would be useful to have simpler models that are crudely accurate and provide simple relationships between deposition rates and resultant steady state densities. Such relationships would highlight the main factors that control the densities of metal species and the functional dependencies involved. For instance, there is no straightforward way to take previously published predictions of metal ion abundances based on the sporadic dust influx and estimate how abundances would change if the entry speed was increased to 56 km s^{-1} while the flux of dust remained unchanged.

The latest models of the cometary dust population predict minimal enhancement of dust influx above sporadic background. However, as Niels Bohr remarked, "prediction is hard, especially about the future," and it remains possible that these latest dust predictions will turn out to be incorrect. The relationships developed in this work can be used to predict the abundances of metal species in the atmosphere should dust estimates change due to, for instance, a cometary outburst. If elevated abundances of metal species are observed in the atmosphere during the encounter, they can also be used to constrain the dust population in the coma.

Acknowledgments

This work was supported, in part, by NASA awards NNX13AH11G and NNX13AO35G. P.W. acknowledges helpful discussion with Tolis Christou, John Moores, and John Plane. P.W. thanks Peter Jenniskens and an anonymous reviewer for helpful comments. No data were used in this paper.

Andrew Dombard thanks Apostolos Christou and Peter Jenniskens for their assistance in evaluating this paper.

References

Barbier, D., and F. E. Roach (1949), Sodium in the upper atmosphere, *Publ. Astron. Soc. Pac.*, *61*, 91–92, doi:10.1086/126134.

Fulle, M., A. C. Levasseur-Regourd, N. McBride, and E. Hadamcik (2000), In situ dust measurements from within the coma of 1P/Halley: First-order approximation with a dust dynamical model, *Astron. J.*, *119*, 1968–1977, doi:10.1086/301285.

Grebowsky, J. M., J. I. Moses, and W. D. Pesnell (2002), Meteoric material—An important component of planetary atmospheres, in *Atmospheres in the Solar System: Comparative Aeronomy, Geophys. Monogr. Ser.,* vol. 130, edited by M. Mendillo, A. F. Nagy, and J. H. Waite, pp. 235–244, AGU, Washington, D. C.

Hughes, D. W. (1992), The meteorite flux, *Space Sci. Rev.*, *61*, 275–299, doi:10.1007/BF00222309.

Jenniskens, P. (2006), *Meteor Showers and Their Parent Comets*, Cambridge Univ. Press, Cambridge, U. K.
Lebedinets, V. N., A. V. Manochina, and V. B. Shushkova (1973), Interaction of the lower thermosphere with the solid component of the interplanetary medium, *Planet. Space Sci.*, *21*, 1317–1332, doi:10.1016/0032-0633(73)90224-9.
Molina-Cuberos, G. J., O. Witasse, J.-P. Lebreton, R. Rodrigo, and J. J. López-Moreno (2003), Meteoric ions in the atmosphere of Mars, *Planet. Space Sci.*, *51*, 239–249.
Molina-Cuberos, J. G., J. J. López-Moreno, and F. Arnold (2008), Meteoric layers in planetary atmospheres, *Space Sci. Rev.*, *137*, 175–191, doi:10.1007/s11214-008-9340-5.
Moores, J. E., T. H. McConnochie, D. W. Ming, P. D. Archer, and A. C. Schuerger (2014), The Siding Spring cometary encounter with Mars: A natural experiment for the Martian atmosphere?, *Geophys. Res. Lett.*, *41*, 4109–4117, doi:10.1002/2014GL060610.
Moorhead, A. V., P. A. Wiegert, and W. J. Cooke (2014), The meteoroid fluence at Mars due to Comet C/2013 A1 (Siding Spring), *Icarus*, *231*, 13–21, doi:10.1016/j.icarus.2013.11.028.
Pätzold, M., P. Edenhofer, M. K. Bird, and H. Volland (1993a), The Giotto encounter with Comet P/Grigg-Skjellerup—First results from the Giotto Radio-Science experiment, *Astron. Astrophys. Lett.*, *268*, 13–16.
Pätzold, M., M. K. Bird, and P. Edenhofer (1993b), The change of Giotto's dynamical state during the P/Grigg-Skjellerup flyby caused by dust particle impacts, *J. Geophys. Res.*, *98*, 20,911–20,920, doi:10.1029/93JA02534.
Pätzold, M., S. Tellmann, B. Häusler, D. Hinson, R. Schaa, and G. L. Tyler (2005), A sporadic third layer in the ionosphere of Mars, *Science*, *310*, 837–839, doi:10.1126/science.1117755.
Pesnell, W. D., and J. Grebowsky (2000), Meteoric magnesium ions in the Martian atmosphere, *J. Geophys. Res.*, *105*, 1695–1708, doi:10.1029/1999JE001115.
Seiff, A., and D. B. Kirk (1977), Structure of the atmosphere of Mars in summer at mid-latitudes, *J. Geophys. Res.*, *82*, 4364–4378.
Tricarico, P., N. H. Samarasinha, M. V. Sykes, J.-Y. Li, T. L. Farnham, M. S. P. Kelley, D. Farnocchia, R. Stevenson, J. M. Bauer, and R. E. Lock (2014), Delivery of dust grains from comet C/2013 A1 (Siding Spring) to Mars, *Astrophys. J. Lett.*, *787*, L35, doi:10.1088/2041-8205/787/2/L35.
Whalley, C. L., and J. M. C. Plane (2010), Meteoric ion layers in the Martian atmosphere, *Faraday Discuss.*, *147*, 349–368, doi:10.1039/c003726e.
Withers, P. (2009), A review of observed variability in the dayside ionosphere of Mars, *Adv. Space Res.*, *44*, 277–307, doi:10.1016/j.asr.2009.04.027.
Withers, P., M. Mendillo, D. P. Hinson, and K. Cahoy (2008), Physical characteristics and occurrence rates of meteoric plasma layers detected in the Martian ionosphere by the Mars Global Surveyor radio science experiment, *J. Geophys. Res.*, *113*, A12314, doi:10.1029/2008JA013636.
Ye, Q.-Z., and M.-T. Hui (2014), An early look of comet C/2013 A1 (Siding Spring): Breathtaker or nightmare?, *Astrophys. J.*, *787*, 115, doi:10.1088/0004-637X/787/2/115.
Yelle, R. V., A. Mahieux, S. Morrison, V. Vuitton, and S. M. Hörst (2014), Perturbation of the Mars atmosphere by the near-collision with Comet C/2013 A1 (Siding Spring), *Icarus*, *237*, 202–210, doi:10.1016/j.icarus.2014.03.030.